33rd Annual International Conference of the IEEE EMBS
Boston, Massachusetts USA, August 30 - September 3, 2011

Detection of Unstained Living Neurospheres from Phase Contrast Images with Very Large Illumination Variations

Wei Xiong, Shue-Ching Chia, Joo-Hwee Lim, Sankaran Shvetha, and Sohail Ahmed

Abstract—**Live imaging of neural stem cells and progenitors is important to follow the biology of these cells. Non-invasive imaging techniques, such as phase contrast microscopy, are preferred as neural stem cells are very sensitive to photoxic damage cause by excitation of fluorescent molecules.However, large illumination variations and weak foreground/background contrast make phase contrast images challenging for image processing. In the current work, we propose a new method to segment neurospheres imaged under phase contrast microscopy by employing high dynamic range imaging and advanced level-set method. The use of high dynamic range imaging enhances the fused image by expressing cell signatures from various exposure captures. We apply advanced level-set method in cell segmentation to improve the detection rate over simple methods such as thresholding. Validation experiments in the analysis of 21 images containing over 400 cells have demonstrated accuracy improvements over existing techniques.**

I. Introduction

Neural stem cells (NSCs) and progenitors (NPs) serve as excellent in vitro models for the central nervous system and the modelling of diseases such as Alzhemier's and Parkinson's. NSCs/NPs can grow in a natural 3D culture system known as neuropsheres. Multiwell plates can be used for neurosphere culture and this combination lends itself for drug screening. Our biologist co-authors (S. Shvetha and S. Ahmed) notice that live NSCs/NPs in neurosphere culture are very sensitive to phototoxic damage and it is not possible to use fluorescence to follow the cells. Hence we propose the use of the non-invasive phase contrast microscopy to follow closely NSCs/NPs.

Phase contrast microscopy converts small phase shifts in the light passing through a transparent specimen into amplitude or contrast changes in the image. In positive phase contrast microscopy, the specimen is visible with medium or dark grey features, surrounded by a bright halo, and the background is of higher intensity than the specimen. In unstained objects, the natural dynamic range is very low as there are limited differences in local brightness, contrast and optical density [1]. Phase contrast images are inevitably contaminated by nonuniform shading artifacts due to the illumination source and the optical influences of the containing wells. As a result, the contaminated images may have large brightness/contrast changes. Fig. 1 shows tiled images from four wells of a 96-well plate automatically acquired in the same batch of a high-content screening experiment with the same illumination and camera exposure settings. Fig. 2 shows two phase contrast images in two different sites of the same well and their thresholding outputs by using Otsu's thresholding method. It is observed that the illumination and shading patterns are rather different from wells to wells and even between images/sites to images/sites within the same well. Obvious failures in dark regions by naive method call for advanced automatic object detection techniques to handle such images which contain large illumination variations.

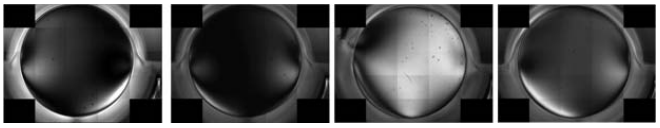

Fig.1. Tiled phase contrast images for four different wells. Nonuniform illumination and serious shading appear in all wells. Some wells are very dark while others are bright.

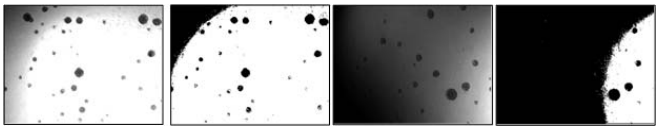

Fig.2. Phase contrast images of unstained neurospheres: (a) and (c) are original images, and (b) and (d) are the thresholded outputs of (a) and (c), respectively.

Many existing techniques make use of the characteristics that cells appear as darker regions surrounded by brighter halos to detect cells in phase contrast microscopy images. A Laplacian of Gaussian based approach is utilized in [2] to detect local extrema and treat them as cell centers. This approach encounters difficulties in our cases as there are multiple foci in a single neurosphere. Ersoy et al. [3] perform cell detection by using ridge measures and a modified geodesic active contour for halo exploration. This method is vulnerable to background distractions as they form local extrema with large intensity curvature. Li et al. [4] also adopt the active contour technique but with a different initialization. All the above methods do not deal with large illumination variations. A preconditioning method is proposed in [5] to preprocess interference-based images with nonuniform shadow-cast artefacts. This method greatly facilitates cell detection but requires careful manual parameter tuning for each cell type and illumination pattern. Moreover, separate illumination/shading corrections have to be made for each

Wei Xiong, Shue-Ching Chia and Joo-Hwee Lim are with Institute for Infocomm Research, A*STAR, Singapore 138632. Sankaran Shvetha and Sohail Ahmed are with Institute of Medical Biology, A*STAR, Singapore 138648. Corresponding author is Wei Xiong: wxiong@i2r,a-star.edu.sg.

shading pattern, making it impractical for high content experiments.

In this work, we propose a new method to handle very large illumination variations for detection of neurospheres. This is based on *digital phase contrast* [1] which utilizes high-dynamic range imaging (HDR) to fuse multiple phase contrast images acquired under different exposure settings [6]. This fusion enables us to enhance all regions in the image space by utilizing various singly-exposed images complementarily. The fused image is then analyzed through a variational level-set technique to segment the neurospheres. Validation experiments have demonstrated improved performance over existing methods utilizing only singly-exposed images.

II. HIGH DYNAMIC RANGE IMAGING

Dynamic range (DR) is the ratio between the largest and the smallest possible values of a changeable quantity. In digital images, an 8-bit image has a low DR equating to 256:1 (LDR). In contrast, a 32-bit image has a high DR equating to 2^{32}:1 (HDR).

The simplest algorithm to create a HDR is to average the LDR images A_i, $i = 1,..,N$, acquired at different exposures, but multiplied by the factor difference between the LDR bit length L and the HDR bit length H. With HDR, one obtains more information than either of the previous images.

In order to generate the largest possible dynamic range (hence most information), a weighted average technique is used. This method emphasizes more on certain input images if their average luminances fall into certain ranges. For example, if an image is pure white, it probably doesn't contain much useful information, so that image should have less impact on the final HDR image [7]. The fused HDR image, B, is

$$B = \frac{1}{N}\sum_{i=1}^{N}(A_i \times 2^{H-L}). \quad (1)$$

To show B in standard 8-bit LDR display devices, tone-mapping techniques are applied to map the HDR image down to 8-bit range. Simply, we can obtain the reconstructed LDR by

$$A = (\left\lfloor \frac{B}{2^{H-1}} \right\rfloor - 1)/2^{L-1}. \quad (2)$$

In the current work, we adapt a method called adaptive gain control with edge detection [7]. In the case where a neighbor pixel is too different in intensity from the pixel being mapped, a counter is incremented and counts the maximum number of pixels that can be too different before the inspected pixel is not mapped at all using the averaged obtained from its neighbors. In this case, the old luminance value is simply assigned to this pixel, which is mapped down to a lower color depth linearly by dividing by the brightest value in the image.

Fig.3 shows two phase contrast images of neurospheres at different exposures (left, middle). They complement with each other and the resultant HDR image (Fig.3 right) is able to bring out cells which would otherwise be too dark or too bright to be observed easily.

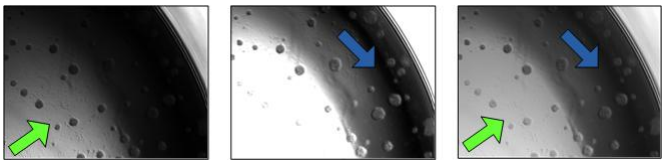

Fig.3. Phase contrast images of neurospheres captured at 100ms exposure (left), 500ms exposure (middle) and the HDR image (right). The green arrow indicates cells seen easily on 100ms exposure image while the blue arrow indicates cells seen easily on the 500ms exposure image. It can be observed that the HDR image is able to bring out cells from both exposures.

III. NEURAL STEM CELLS/NEUROSPHERES DETECTION METHODOLOGY

We now introduce our neurosphere detection method. The naïve high content screening imaging protocol is modified to acquire phase contrast images at various exposures. Our method (**M0**) comprises of three main steps. The first step creates a HDR image by combining multiple-exposure images at the same sites by using the methods described above. The second step performs a background subtraction which will reduce the effect of uneven background illumination. The final step segments out the cells by applying the level set method.

Phase contrast microscopy cell images present a challenge in segmentation due to the presence of severe uneven background illumination. In order to offset this problem, we apply a simple background subtraction technique to the HDR images before performing segmentation. We first apply Gaussian blur on the HDR image and then use the same HDR image to subtract away the blurred image. The resultant image will be the background subtracted image. In general, we observe that images with background subtraction give better segmentation results compared to images without background subtraction.

The level set segmentation technique is an active contour approach which evolves an initial close contour/surface according to a rate change partial differential equation. The contour/surface is embedded as the zero level-set of a higher dimensional implicit function. The evolution can naturally split or merge contours and converges to high gradient parts subject to data constraints [8]. We adopt a variational level-set approach which does not require re-initializations [9] for the segmentation of neurospheres and employed the boundary of the entire image region as the initialization of the active contour.

IV. EXPERIMENTS AND RESULTS

In our experiments, a well is covered by 5x5 sites and only 21 sites are imaged without the four corners. We have imaged each site under three different exposures, 30ms, 100ms and 500ms respectively. Fig. 4 shows the tiled 21 images in a well

with an exposure of 100ms. Due to optical artifacts, a consistent dark circular band can be observed around the perimeter of the well with some irregular shading. The ground truths for these images are labeled manually. According to domain experts, objects smaller than 64 pixels (8x8) are ignored as these are not likely to be neurospheres formed by the proliferation of neural stem cells. Excluding these small objects, there are 446 neurospheres in this well shown in Fig. 4. The images (size: 464×364) in the 21 sites are used to verify our methods. In our experiments, we use the weighted average method and set the high dynamic range bit length as 32 in the creation of HDR images. For background subtraction, we use a Gaussian blur with window size = 7x7 and sigma = 2.

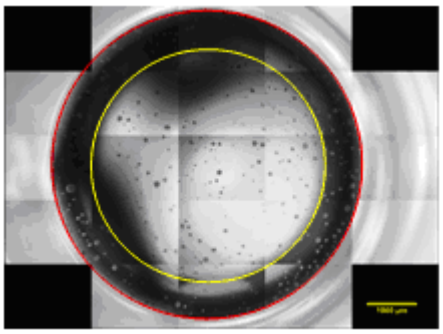

Fig.4. A consistent dark circular band can be observed around the perimeter of the well. The red marking indicates the full well. The yellow marking indicates the brighter inner circle which excludes the dark circular band from the full well.

We compared **M0** with four other methods. For the first (**M1**) and second method (**M2**), we perform level-set directly on the original images at 100ms and 500ms exposure respectively. For the third method (**M3**), a variation of **M0,** we apply level-set on the HDR image without background subtraction. In all the level-set based segmentation approaches, we use the same default parameters suggested by [9] with maximum 10,000 iterations and the entire image region is set as the initial contour. In the last method (**M4**), we apply Otsu thresholding on the original image at 100ms exposure.

In Fig. 5 we show segmentation results of one of the images. The red contours delineate the segmented neurospheres. It is obvious that **M0** achieved the best segmentation. **M1, M2** and **M4**, which process the single-exposure image, respectively, cannot segment the neurospheres properly. **M3**, on the other hand, can detect some but with certain errors.

Fig. 6 illustrates the tiled segmentation results of the five methods. The blue markers outlined the contours of the cells labeled in the ground truth and the yellow markers outlined the segmentation results by each method. If the segmented neurosphere happens to be exactly the same as the ground truth, it is marked in yellow. Visually, we observe that **M0** performs the best in all sites among the five methods. However, almost all the methods have difficulties in segmenting objects in the dark ring.

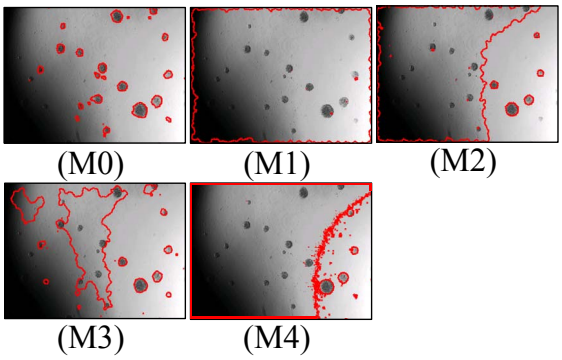

Fig.5. Comparison of segmentation results between **M0**, **M1**, **M2**, **M3** and **M4**. The red markers indicate the segmentation contours by each method.

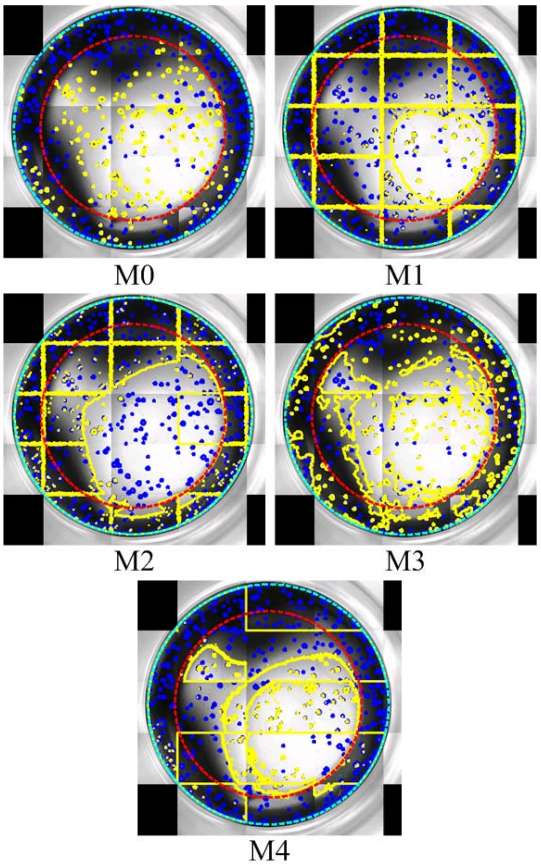

Fig.6. Tiled segmentation results of **M0**, **M1**, **M2**, **M3** and **M4**. The blue markers outlined the contours of the cells labeled in the ground truth, while the yellow markers outlined the segmentation results. The cyan dotted ring outlined the region of interest of the full well. The red dotted ring outlined the region of interest of the brighter inner region which excludes the dark circular band around the perimeter of the well.

For quantifiable evaluations, we compute the sensitivity, specificity and positive prediction value (PPV) for each method. To facilitate on the computation of the metrics, we state the following definitions. Positive (P) is the set of

foreground pixels in the ground truth. Negative (N) is the set of background pixels. True Positive (TP) is the set of foreground pixels in both the segmented result and the ground truth. False Positive (FP) is the set of foreground pixels which exists in the segmented result but not in the ground truth. False Negative (FN) is the set of foreground pixels which exists in the ground truth but not the segmented result. True Negative (TN) is $N - FP$. Therefore, sensitivity = $TP/(TP + FN)$, specificity = $TN/(FP + TN)$ and PPV = $TP/(TP + FP)$. A perfect segmentation gives 100% for all 3 metrics.

Table 1 shows the first set of result which considers only the brighter circular region in the middle of the well and excludes the dark band along the perimeter of the well (Fig.4). The second set of metrics computes for the entire full well and is presented in Table 2. From Table 1, we can observe that **M0** generally performs better than other methods, with a sensitivity of 98.98%, a specificity of 66.62% and a positive prediction value of 67.36%. From Table 2, although **M0** still performs reasonably better than other methods, the result is not as favorable as compared to Table 1 as its specificity (36.64%) is lower. The main reason for this is because **M0** and all other methods are unable to detect most of the cells that reside in the dark band along the perimeter of the well wall. From Table 2, we can also observe that M3 offers comparable sensitivity and specificity against M0. But its low PPV suggests a high false positive rate and hence our preference of M0 over M3.

Table1. Comparison results for only the brighter circular region in the middle of the well.

	Sensitivity (%)	Specificity (%)	PPV (%)
M0	98.98	66.62	67.36
M1	47.30	88.57	5.02
M2	65.62	54.75	4.77
M3	87.07	74.73	15.39
M4	59.09	57.66	4.24

Table2. Comparison results for the entire well.

	Sensitivity (%)	Specificity (%)	PPV (%)
M0	99.58	36.64	72.28
M1	60.26	91.72	6.50
M2	69.27	73.78	6.74
M3	92.62	65.57	21.12
M4	72.29	59.01	6.03

V. DISCUSSIONS AND CONCLUSIONS

To follow live NSCs/NPs in neurosphere culture with phase contrast microscopy requires the development of new image processing techniques. Here we show that digital phase contrast followed by advanced image processing can be used to overcome the problem of uneven background illumination and to segment the neurospheres. Qualitatively, high dynamic range imaging enhances the image quality and level-set method improves the accuracy. Our method has been validated by analyzing over 400 cells with improved accuracy over existing techniques. One of our future works is to further improve on the detection rate for cells that reside in the low illumination regions and exhibit weak signatures.

ACKNOWLEDGMENT

We would like to thank Dr. Lee Hwee Kuan (with Bioinformatics Institute, Singapore) for his help in this work. This work is supported in part by Agency for Science, Technology and Research, Joint Council Office under grant number JCOAG03_FG01_2009.

REFERENCES

[1] Jörg Piper, "Ultra-high contrast amplification in bright-field images," in *Microscopy Today*, 2010, vol.18, no. 3, pp. 10-16.

[2] M. Usaj, D. Torkar, and D. Miklavcic, "Automatic cell detection in phase-contrast images for evaluation of electroporation efficiency in vitro," in Proc. *of the 11th Mediterranean Conference on Medical and Biomedical Engineering and Computing*, 2007, pp. 851–855.

[3] I. Ersoy, F. Bunyak, M.A. Mackey, and K. Palaniappan, "Cell segmentation using Hessian-based detection and contour evolution with directional derivatives," in Proc. of *International Conference on Image Processing*, 2008. pp. 1804-1807.

[4] Fuhai Li, Xiaobo Zhou, Hong Zhao, and Stephen T.C. Wong, "Cell segmentation using front vector flow guided active contours," *Medical Image Computing in Computer Assisted Intervention*, 2009, vol. 12 No. pt2, pp. 609-616.

[5] K. Li, and T. Kanade, "Nonnegative mixed-norm preconditioning for microscopy image segmentation," in *Proc. of the 21st Biennial International Conference on Information Processing in Medical Imaging*, 2009. 21, pp. 362-373,

[6] Reinhard, Erik; Ward, Greg; Pattanaik, Sumanta; Debevec, Paul (2006). *High dynamic range imaging: acquisition, display, and image-based lighting*. Amsterdam: Elsevier/Morgan Kaufmann

[7] Yang, Tianhe, Taylor Johnson, Robert Ortman, and Sarah McGee, "Exploring High Dynamic Range Imaging" Connexions. Retrieval on December 25, 2006. http://cnx.org/content/m14237/1.2/.

[8] Chan, T.F., Vese, L.A., "Active contours without edges". IEEE Transactions on Image Processing, Feb 2001, Vol 10, No 2, pg 266-277

[9] Chunming Li, Chenyang Xu, Changfeng Gui and Martin D. Fox, "Level Set Evolution Without Re-initialization: A New Variational Formulation". IEEE International Conference on Computer Vision and Pattern Recognition (CVPR), vol. 1, pp. 430-436, San Diego, 2005